Int. J. Electrochem. Sci., 11 **(2016)** 915 - 928

International Journal of
ELECTROCHEMICAL
SCIENCE
www.electrochemsci.org

The Formation and Characterization of Copper Telluride Films from Choline Chloride – Urea Ionic Liquid

Florentina Golgovici[1], *Adriana-Simona Catrangiu*[1,*], *Teodor Visan*[1]

Faculty of Applied Chemistry and Materials Science, University POLITEHNICA of Bucharest, Bucharest, Romania.
[*]E-mail: adriana_catrangiu@yahoo.com

Received: 10 July 2015 / *Accepted:* 23 November 2015 / *Published:* 1 January 2016

Copper telluride electrodeposition on platinum in ionic liquid media at 60^0C is reported. The background electrolyte as solvent ionic liquid consisted in an eutectic mixture of choline chloride and urea (1:2 mole ratio) in which 5-20 mM CuCl and 8 mM TeO_2 were dissolved. Cyclic voltammetry and electrochemical impedance spectroscopy using Pt electrode were applied for investigating the corresponding electrode processes. The electrochemical studies have permitted to interpret the sequence of the Cu metal and Cu_xTe semiconductor compound depositions and their anodic dissolution. AFM microscopy is also used to determine thickness and roughness of deposited Cu_xTe films.

Keywords: Copper Telluride; Electrodeposition; Ionic Liquids; Choline Chloride – Urea Eutectic

1. INTRODUCTION

Metal tellurides as binary or ternary compounds are of particular interest due their broad range of band-gaps, as well as the wide variety of properties that make them competing candidates for other semiconductor materials in thermoelectricity, energy conversion and optoelectronic applications. Copper tellurides (Cu_xTe, for $1<x<2$) are usually p-type semiconductors, suitable for applications in solar cells (including ohmic contacts to CdS/CdTe photovoltaic devices), photodetectors, electroconductive electrodes and other advanced electronic applications such as for microwave shielding coating and nonvolatile memories [1-5].

The electrodeposition technique has gained much attention for the production of thin films or nanostructures, widely used in photovoltaic and optoelectronic devices, since the electrochemical deposition enables much simpler technology and less expensive fabrication process [6]. Copper tellurides are generally electrodeposited from aqueous solutions containing dissolved chlorides [7],

sulfates [8-11] or nitrates [12]. However, it is difficult in such media to prevent hydrogen evolution, which leads to the low current efficiency and worse quality of deposits due to the hydrogen embrittlement.

Ionic liquids are a new kind of solvents that can be used as promising non-aqueous electrolytes for the electrodeposition of thin films and nanostructures [6,13-15]. They are the ideal alternative electrolytes for electrodeposition of various metals, alloys and semiconductor compounds since they possess properties such as wide electrochemical window, negligible vapor pressure, good electrical conductivity and low melting point. This may explain the use of traditional room temperature ionic liquids containing acidic chloroaluminate, imidazolium or pyrrolidinium derivatives for the deposition of copper metal [16-24].

However, in recent years many research groups have found that binary mixtures containing choline chloride (*hydroxy-ethyl-trimethyl ammonium chloride*, ChCl) are expected to be preferable for electrodeposition of various metals or semiconductors because these ionic liquid analogues (called also Deep Eutectic Solvents) show good ability to dissolve many metal compounds, are air and water stable and relatively inexpensive as well as environmental friendly [25-33]. To prepare such DES, choline chloride is mixed with a hydrogen bond donor such as an amide (urea), alcohol (ethylene glycol) or carboxylic acid (malonic acid, oxalic acid). We found that copper telluride electrodeposition has not been reported in this kind of ionic liquids, except some papers that discuss the copper and copper alloys electrodeposition [34-44].

In this work we investigated the electrode processes of co-reduction of Cu^{+} and Te^{4+} ions in choline chloride – urea ionic liquid in order to prepare copper telluride films by electrodeposition. To our best knowledge, the present study is a first work in such ionic liquid concerning the Cu and Te codeposition. The ionic liquid analogue used in this work is based on the ChCl-urea (1:2 mole ratio) mixture, for which previous FTIR spectroscopy and electrochemical studies [33,45] have demonstrated its special characteristic features.

2. EXPERIMENTAL PART

The background electrolyte was prepared using a mixture of choline chloride with urea (both reagents from Aldrich, without being recrystallized or dried) and heating the two components in 1:2 molar proportions at above 80^0C for more than 30 min to achieve a homogeneous colourless liquid. CuCl (Aldrich) and TeO_2 (Alfa Aesar) reagents, as precursors of Cu^{+} and Te^{4+} ions, were also used as received, being dissolved in the ChCl-urea solvent. In order to calculate the solution molarities we used a density value of ChCl-urea of 1.13398 gcm^{-3}, determined in our laboratory at 60 ^{o}C working temperature.

During the study of cathodic/anodic processes in a cell with one single compartment, a platinum sheet was used as working electrode, whereas the auxiliary electrode was a platinum mesh with large area. A silver wire immersed in the working electrolyte containing copper and tellurium ions was the quasi-reference electrode. The Pt working electrode was polished with alumina paste, cleaned in water and dried before every measurement. A Metrohm / Eco Chemie Autolab PGSTAT 12

potentiostat provided with a frequency response analyzer was used and cyclic voltammetry (CV) and electrochemical impedance spectroscopy (EIS) measurements were carried out. Cyclic voltammograms were recorded at scan rates from 2 to 100 mVs^{-1}. Electrochemical impedance spectroscopy (EIS) for obtaining Nyquist and Bode spectra was carried out in the 10^{-1} Hz < f < 10^{5} Hz frequency range with an *ac* voltage amplitude of ±10 mV. The *ac* signal is applied together with gradually polarizing Pt cathode, typically in the potential range of 0 V to -0.8 V (vs. Ag quasi-reference electrode).

Cu_xTe films were electrodeposited in potentiostatic conditions on Pt sheets in ChCl-urea (1:2) eutectic based baths, in stagnant conditions. The cathode had an exposed area of 3-4 cm^2 and was located vertically; a parallel Pt sheet was used as anode in the cell. All samples were obtained at constant temperature (60 ^{o}C). The samples I and II were deposited at -0.5 V from 10 mM CuCl + 8 mM TeO_2 contained electrolyte for 30 and 60 minutes, respectively. The samples III and IV were deposited from 20 mM CuCl + 8 mM TeO_2 contained electrolyte, 60 minutes, at -0.5 V (sample III) and -0.4 V (sample IV). Film thickness and roughness were determined by using an AFM microscope type A100-SGS from A.P.E. Research, Italy. The AFM micrographies were analyzed using a Gwyddion 2.20 data visualization and analysis software.

3. RESULTS AND DISCUSSION

3.1. CV and EIS Investigations of the Electrodeposition/Electrodissolution Processes

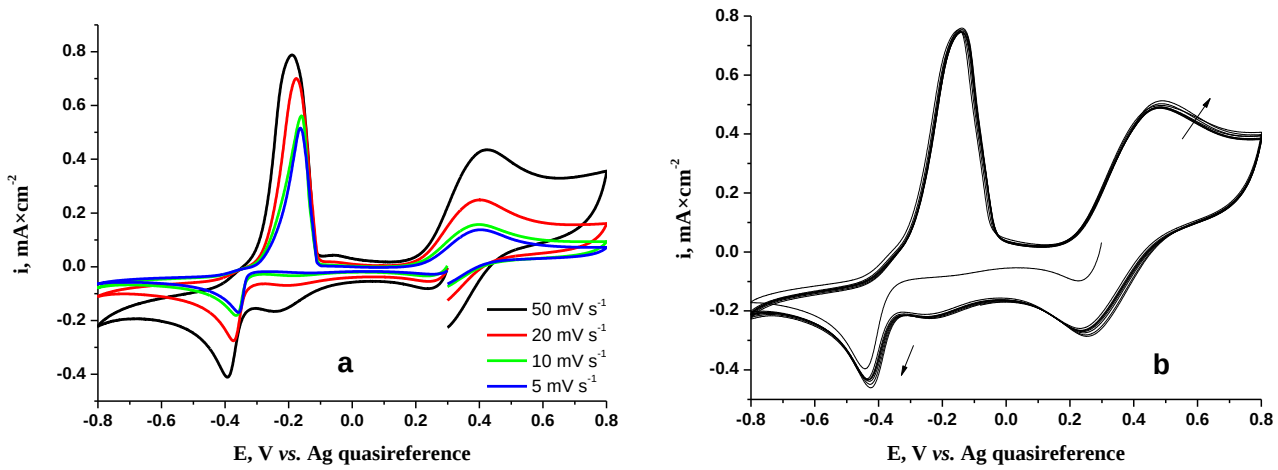

Figure 1. Cyclic voltammograms (CVs) on Pt in ChCl-urea + 10 mM CuCl + 8 mM TeO_2, 60 ^{o}C: (a) CVs for various scan rates; (b) The first five repetitive CVs with 100 mVs^{-1} scan rate

Cyclic voltammetry has been first used to provide information about the sequence of processes involved at different potentials during the potential scan. Cyclic voltammetry curves (CVs) of the ChCl-urea ionic liquid solvent without metal precursors were previously plotted by different authors [33, 41, 46]. We found out in such curves at 60-80 ^{o}C electrochemical windows of 2.1-2.2 V using Pt electrode, determined as a difference between cathodic and anodic limits. They

become larger if the scan rate is increased (in the range 5-200 mVs^{-1}) and this influence was monotonous.

The typical cyclic voltammetry behavior of ChCl-urea + 10 mM CuCl + 8 mM TeO_2 ionic liquid is shown in Fig. 1.

Scanning toward negative potentials during recording cyclic voltammograms, from 0.3 V up to -0.8 V and back, three reduction peaks and three oxidation peaks can be seen, as Fig. 1a shows. In order to explain the shape of these CVs we mention that in the literature regarding cyclic voltammetry of copper ions it is generally accepted that an equilibrium between Cu^{2+} and Cu^{+} is established whatever mono- or divalent copper salt is dissolved into electrolyte. This seems to be the case of ChCl-urea ionic liquid, too [41], although the Cu^{2+} concentration is probably very low compared to Cu^{+} concentration introduced by dissolving CuCl precursor salt. Therefore, we can attribute the cathodic peak (located at 0.25 V), that appears even in the beginning of scan, to the Cu^{2+}/Cu^{+} redox process which is well reproduced in the repetitive scans (Fig. 1b). The peak at -0.25 V or the plateau of current that begins at -0.1 V are associated with Te underpotential deposition process, Te-UPD, meaning a four-electron transfer to Te^{4+}. By continuing more negatively the potential scan Figures 1 show the main cathodic peak in the region from -0.35 to -0.4 V. We suppose that copper metal deposition and Cu-Te co-deposition take place simultaneously on the working electrode surface (processes 1 and 2). We mention that CVs curves obtained by other authors in ionic liquids [16, 18, 41, 43] have shown similar reduction peaks for Cu^{+} in the same potential region, being more pronounced on Pt than on glassy carbon electrode.

Nevertheless, it is possible to occur a surface reaction (process 3) of Te obtained by UPD and Cu^{+} ions. The following equations were proposed for the electrode processes:

$$Cu^{+} + e^{-} \rightarrow Cu \quad (1)$$

$$x\,Cu^{+} + Te^{4+} + (4+x)\,e^{-} \rightarrow Cu_xTe \quad (2)$$

$$x\,Cu^{+} + Te + x\,e^{-} \rightarrow Cu_xTe \quad (3)$$

As can be seen, we proposed two alternative mechanisms for Cu_xTe formation either by direct co-reduction of both Cu^{+} and Te^{4+} ions existing in electrolyte (most possible process) or by a reaction of Cu^{+} with Te film already deposited on the Pt surface. This deposition couple of cathodic processes continues at more negative potentials as limiting current after the main peak.

Anodic branches of CV curves exhibit a sequence of three processes assigned to electrochemical dissolution of both Cu_xTe and Cu (the well pronounced peak at -0.2 V), to dissolution of Te-UPD monolayer (the small anodic peak or wave at 0 V), and to Cu^{+}/Cu^{2+} oxidation process (the broad peak at around 0.4 V), respectively. On the five repetitive CVs in Fig. 1b a stationary shape is observed that was reached even at the second scan. This Figure shows clearly the Cu^{+}/Cu^{2+} couple which is a homogeneous redox couple in the ionic liquid.

The corresponding EIS diagrams for ChCl-urea + 10 mM CuCl + 8 mM TeO_2 electrolyte are presented in Figures 2.

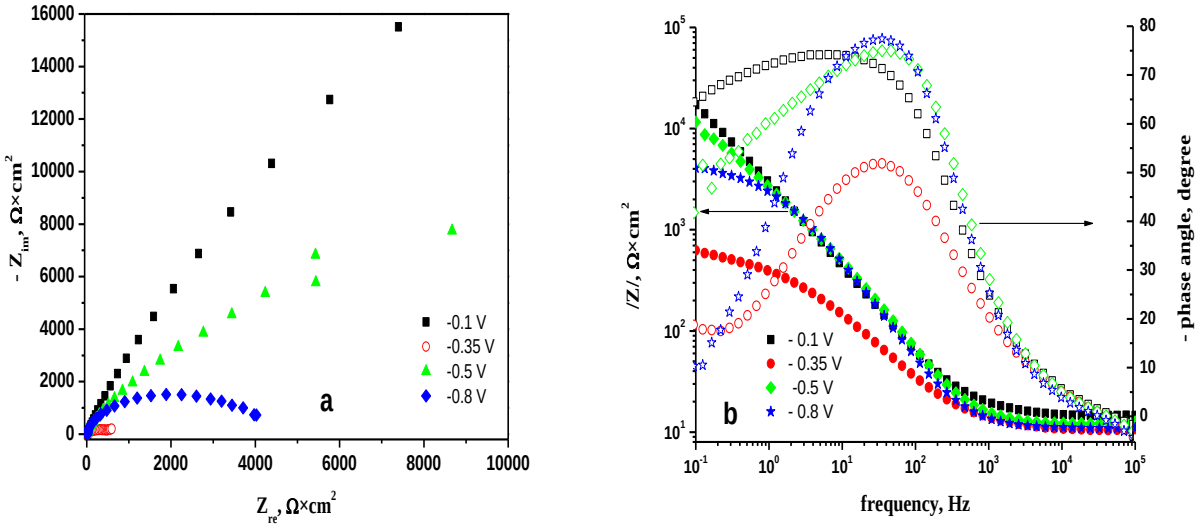

Figure 2. Nyquist (a) and Bode (b) spectra on Pt in ChCl-urea +10 mM CuCl + 8 mM TeO_2, 60 ^oC,at polarization with various applied potentials

Fig. 2a presents comparatively Nyquist impedance spectra at different polarization potentials, selected in the range of cathodic processes of interest. Thus, the impedance results are interpreted in relation with voltammetric results.

The changes of the Nyquist semicircle diameter with different polarization of the electrode confirm the successive steps in the cathodic direction. They should be interpreted taking into account that the diameter corresponds to the charge-transfer resistance which is inversely correlated to the process rate: the larger the charge-transfer resistance, the lower is the rate of faradaic reaction. Thus, the largest semicircle for -0.1 V polarization corresponds to Te-UPD process as a first deposition step with a slow rate due to formation of Te semiconductor film. Correspondingly, the maximum phase angle in Bode diagram has a very high negative value (-74^o). Further, the sudden decrease of Nyquist diameter at -0.35 V polarization is attributed to the simultaneous Cu deposition and CuTe codeposition. At this polarization potential aproximately equal to peak potential in CV curves, the electrolysis current (i.e. reaction rate) is the highest. This is indicated by the smallest Nyquist diameter and also by the smallest value (-50^o) of maximum phase angle in the Bode diagram. The following more negative polarizations lead to gradual decreasing of electrolysis current and the gradual increase of Bode phase angle due to a thickenning of Cu_xTe semiconductor; it is probably that a Te-rich Cu_xTe semiconductor deposit is formed at excessive negative polarization.

In the following the electrochemical behavior of Cu^+ and Te^{4+} mixtures in the ChCl-urea solvent was examined by cyclic voltammetry carried out at other different concentrations of Cu^+, by keeping constant Te^{4+} concentration. The obtained results are shown in Figures 3-5. A sequence of three cathodic and anodic peaks is also observed and the results were similarly interpreted as in CVs from Fig. 1. Thus, the cathodic peaks were assigned successively to Cu^{2+}/Cu^+ homogeneous reduction, Te-UPD process, and simultaneous deposition of Cu and Cu_xTe, with peak potentials having almost similar values as for 10 mM CuCl + 8 mM TeO_2 mixture.

The CVs from Fig. 3b show the influences to voltammogram shape of cathodic limit where the scan is reversed. Different negative limits of scanning were tested. Only a single redox couple (Cu^{+}/Cu^{2+}) occurs on curve 1, whereas a supplementary cathodic process (of Te-UPD) is observed on curve 2. The curve 3 (thicker line) indicates the begining of Cu metal deposition, which is followed at scan reversing by a clear anodic peak of electrochemical dissolution. Curve 4 is recorded along the cathodic region where both Cu deposition and Cu_xTe deposition occur, so that the anodic response in this case is a wide anodic peak attributed to dissolution of both kinds of microcrystals. Certainly, the stoichiometry of Cu_xTe deposit gradually changes with decreasing the Cu^{+} content in the electrolyte, leading to a semiconductor more enriched in Te. Finally, the extended curve 5 indicates the additional process of cholinium ion (from solvent) reduction as a limiting current at the excessive negative potentials. Figure 4b indicates that all processes are well reproduced in the repetitive scans.

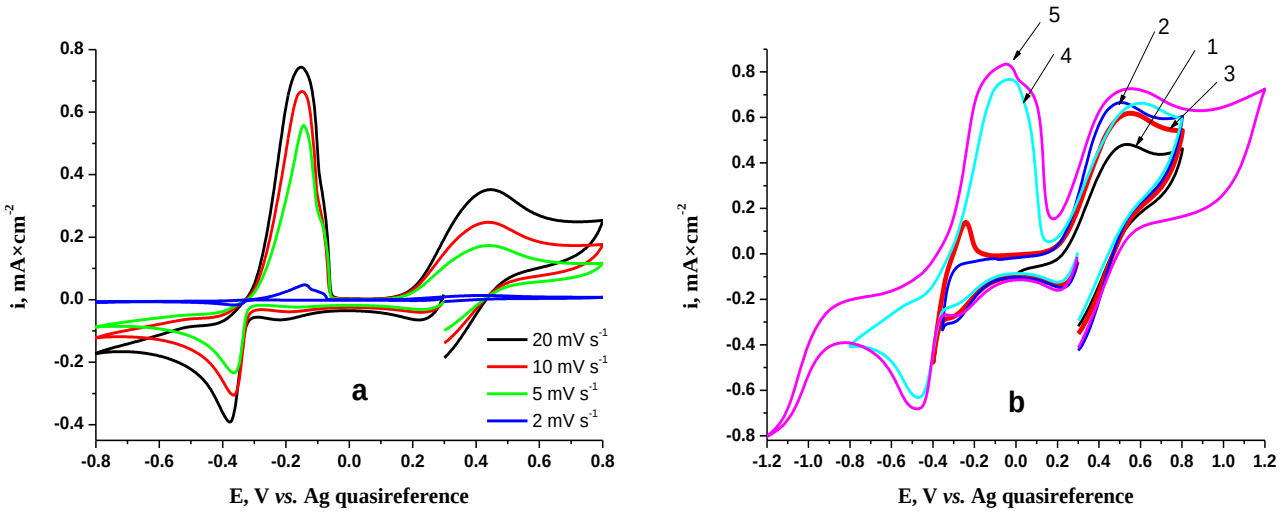

Figure 3. CVs on Pt in ChCl-urea + 20 mM CuCl + 8 mM TeO_2, 60 ^{o}C: (a) CVs with various scan rates; (b) CVs with 100 mVs^{-1} scan rate showing the influence of cathodic limit: (1) up to 0 V: (2) up to -0.35 V; (3) up to -0.4 V; (4) up to -0.8 V; (5) up to -1.2 V

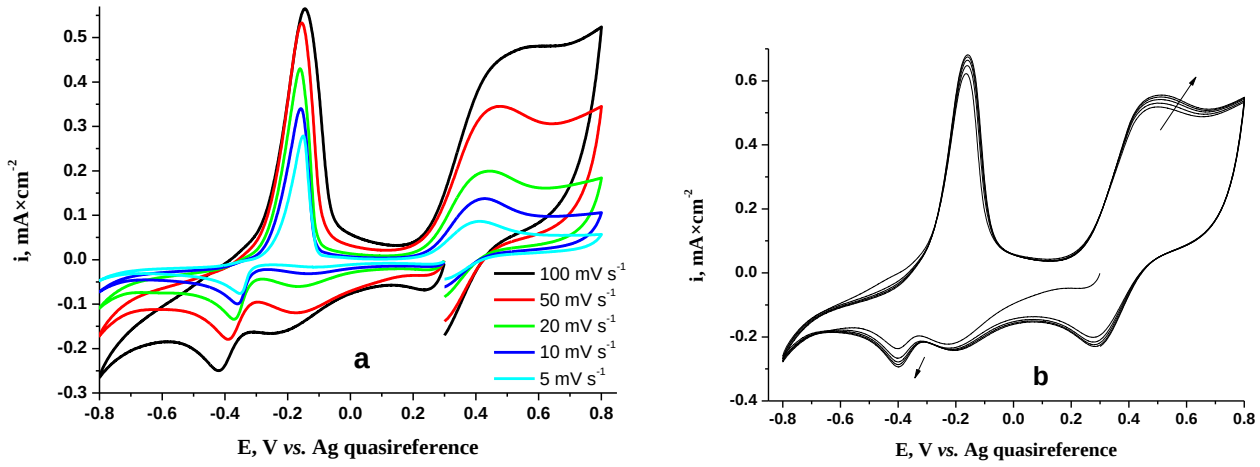

Figure 4. CVs on Pt in ChCl-urea + 5 mM CuCl + 8 mM TeO_2, 60 ^{o}C: (a) CVs with various scan rates; (b) the first five repetitive CVs with 100 mVs^{-1} scan rate

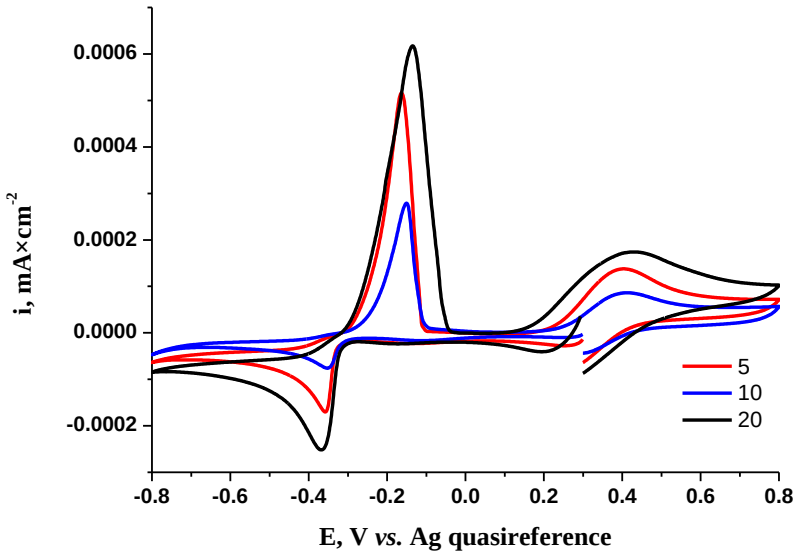

Figure 5. Comparative CVs on Pt in ChCl-urea + x mM CuCl + 8 mM TeO_2 ionic liquids, 60 ^oC, 5 mVs^{-1}scan rate; CuCl concentrations: 5; 10 and 20 mM

Comparative voltammograms from Figure 5 show a small shift of peak potentials for deposition/stripping dissolution of Cu+Cu_xTe deposit, especially for cathodic peak. This may suggest a quasireversible process from electrochemical point of view. However, we believe that the potential shift can be due partially to a high uncompensated ohmic drop existing in viscous ionic liquid media.

We have determined for the currents of the main cathodic and anodic peaks in Figure 5 a linear increase with CuCl concentration indicating that the processes are diffusion controlled. The diffusion control is also demonstrated by representing the plots of peak current (i_p) *versus* the square root of scan rate ($v^{1/2}$). Figure 6 shows some examples of the corresponding i_p–$v^{1/2}$ linear dependences for the process of simultaneous deposition of Cu metal and Cu_xTe compound in choline chloride – urea electrolytes containing 8 mM TeO_2 and various CuCl concentrantions. Certainly, all straight lines do not pass through origin due to the complexity of cathodic mechanism.

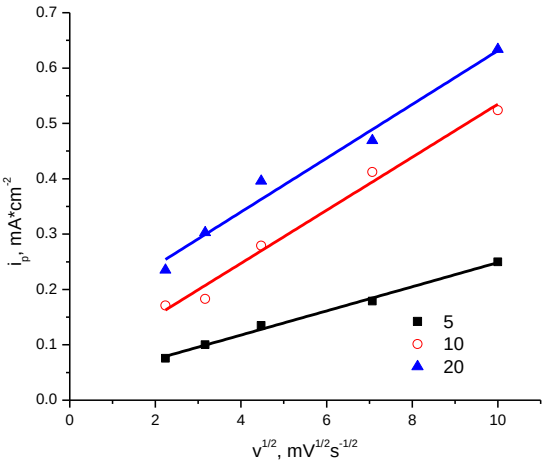

Figure 6. i_p–$v^{1/2}$ plots in ChCl-urea + x mM CuCl + 8 mM TeO_2 ionic liquids, 60 ^oC.CuCl concentrations (x): 5; 10 and 20 mM

Figures 7 and 8 present the impedance spectra (as Nyquist and Bode diagrams) for 20 mM Cu^{+} + 8 mM Te^{4+} and 5 mM Cu^{+} + 8 mM Te^{4+} mixtures, both CuCl and TeO_2 being dissolved in ChCl-urea solvent. Some comparative EIS spectra for the three CuCl millimolar concentrations, as examples for the Pt behavior at polarization within the potential region of Cu and Cu_xTe depositions, were given in Figures 9.

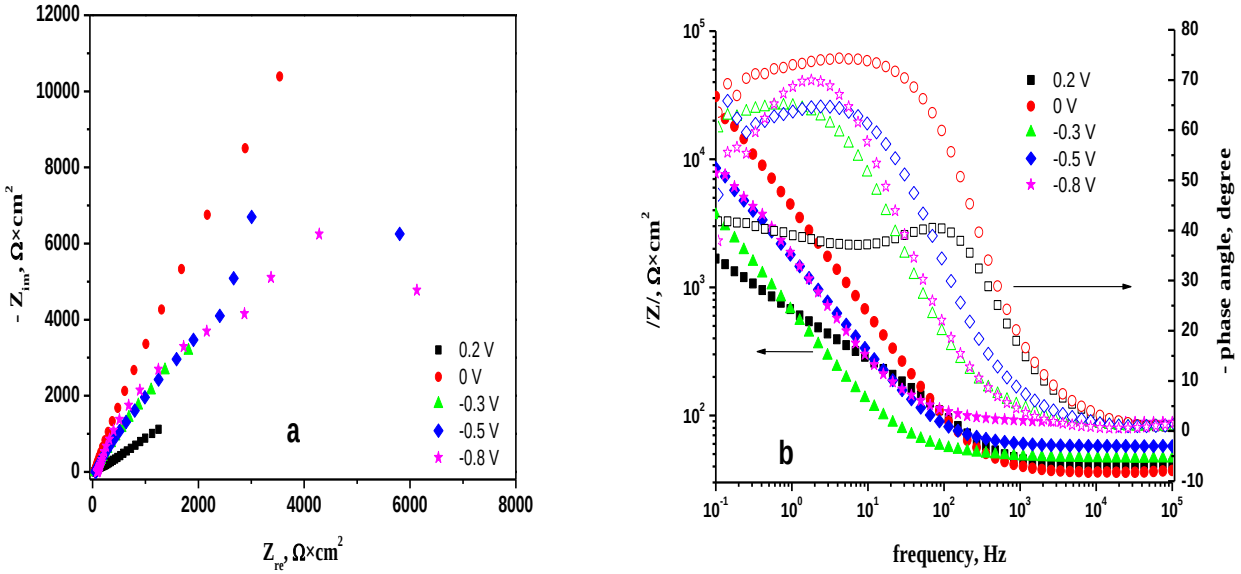

Figure 7. Nyquist (a) and Bode (b) spectra on Pt in ChCl-urea + 20 mM CuCl + 8 mM TeO_2, 60 ^{o}C,at polarization with various applied potentials.

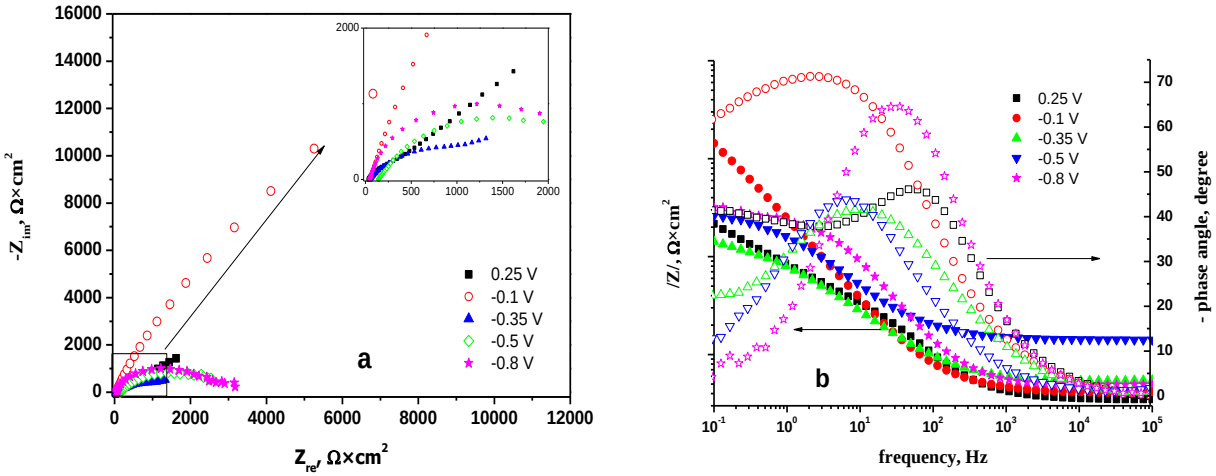

Figure 8. Nyquist (a) and Bode (b) spectra on Pt in ChCl-urea + 5 mM CuCl + 8 mM TeO_2,60 ^{o}C, at polarization with various applied potentials.

For all EIS curves the evolution of shape with polarization potential confirms the cyclic voltammetric results. Thus, Fig. 7a shows a sudden increase of semicircle diameter due to Te-UPD process that begins at 0 V; the corresponding maximum phase angle (Fig. 7b) is the highest (-74^{o}) due

to semiconductor Te element. It follows an approximately constancy in the Nyquist diameter at polarization from -0.3 to -0.8 V indicating a constant electrolysis rate; as a consequence, the continuous thickening of Cu_xTe deposit is illustrated by gradual increase of Bode phase angle when the polarization potential is -0.8 V.

For the electrolyte system which is richer in Te^{4+} than in Cu^+ content (5 mM CuCl + 8 mM TeO_2), Fig. 8a shows also a dramatical increase of semicircle diameter at -0.1 V polarization due to Te-UPD process that begins at -0.1 V. Similarly to Fig. 7b, Fig. 8b presents the highest maximum phase angle (-72^o) due to deposition of semiconductor Te element. However, at further negative polarization the Nyquist diameter decreases, an explanation being the excess of Te content in the Cu_xTe deposit. Tellurium element has a lower electrical conductivity than metallic copper, and thus the Bode phase angle increase from -45^o to -65^o (see Fig. 8b) may be explained.

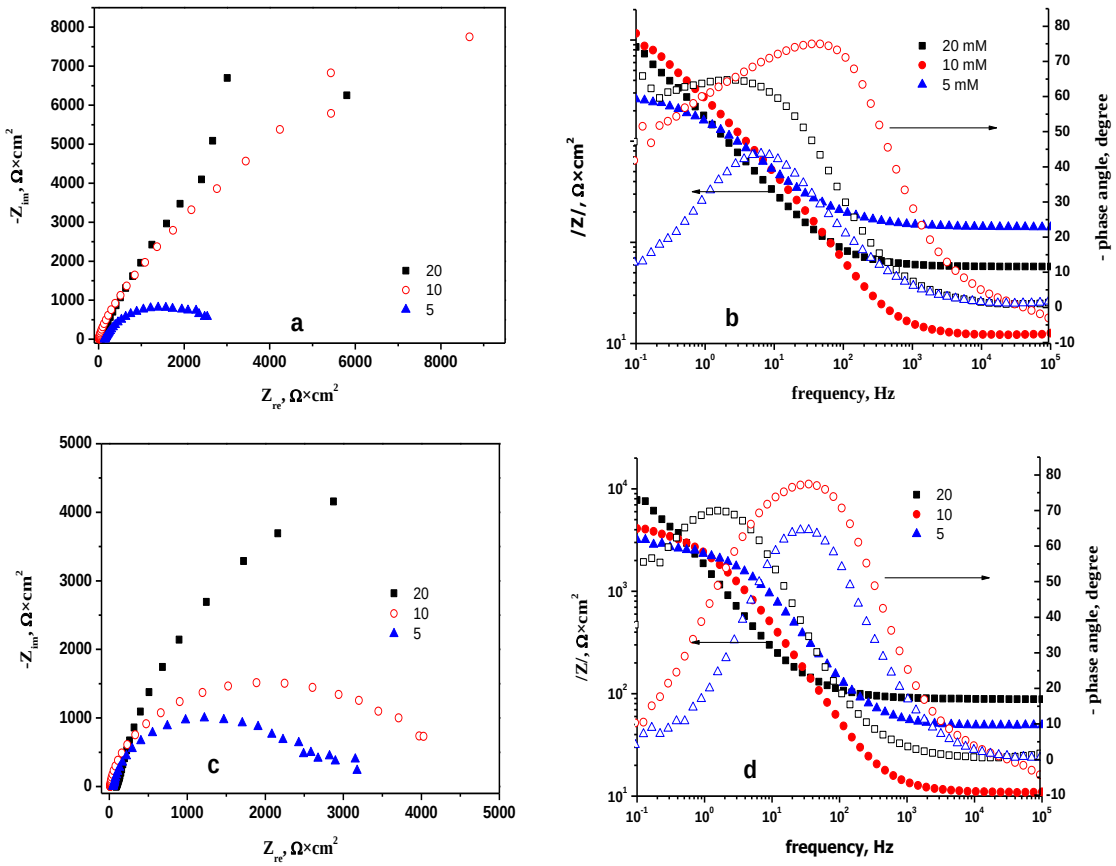

Figure 9. Comparative Nyquist (a,c) and Bode (b,d) spectra on Pt in ChCl-urea + x mM CuCl + 8 mM TeO_2 ionic liquids (x=5, 10 and 20 mM CuCl), 60 ^{o}C; potential values of -0.5 V (a,b) and -0.8 V (c,d) for applied polarization.

The EIS spectra presented in Figures 9 show the evolution of the impedance parameters with the Cu^+ concentration increase at -0.5 V and -0.8 V polarization. Clearly, for both polarization potentials the Nyquist semicircles increase gradually in diameter with Cu^+ concentration. Neverthess, there are some different variations regarding values of the impedance modulus and maximum phase angle. As Figs. 9b and 9d show, the maximum phase angle has the highest values (around -75^o) for the 10 mM CuCl + 8 mM TeO_2 electrolyte, indicating that this ionic liquid favors the formation of Cu_xTe

compound with a particular stoichiometry (Cu_2Te, probably) which ensures very good semiconductive properties.

3.2. AFM Characterization of the Electrodeposited Cu_xTe Films

Cu_xTe films were potentiostatically electrodeposited from electrolytes with 10 mM CuCl + 8 mM TeO_2 and 20 mM CuCl + 8 mM TeO_2 concentrations in the choline chloride – urea solvent. The electrolysis was carried out for 30 or 60 minutes at 60 °C to deposit thin Cu_xTe films on Pt substrate. The operating conditions (bath composition, applied potential and deposition time) for the investigated samples are listed in Table 1. The averaged values of film thickness and the roughness values determined by atomic force microscopy were also listed in this Table. A comparison of samples I and II shows a proportional increase of Cu_xTe film thickness with electrolysis time, indicating a constancy of growth rate during the first hour of electrolysis. However, the thickness of film from sample III is two times greater than from sample II, meaning that an increase of Cu^+ content in the bath led to higher growth rate. Also, a different behavior regarding the growth rate is observed for film of sample IV prepared at less negative polarization potential than for sample III; the thinner Cu_xTe film obtained for this sample may be due to the decreased current during electrolysis time at -0.4 V polarization which is different than the evolution of current at -0.5 V. In general, the obtained values of roughness parameters with the same order of magnitude indicate a quite better behavior for samples deposited from ChCl-urea + CuCl + TeO_2 ionic liquids.

Table 1. AFM data regarding thickness and roughness values (Ra -arithmetic average and Rms –root mean squared average) of Cu_xTe films deposited on Pt, from ChCl-urea + CuCl + TeO_2ionic liquids at 60 ^oC

Sample /Potentio-static control	Operation conditions			Thickness (averaged), nm	Roughness	
	Cu^+ and Te^{4+} concs.	Controlled potential (vs. Ag)	Electrolysis time, min		Ra, nm	Rms, nm
Sample I	10 mM CuCl + 8 mM TeO_2	E= -0.5 V	30	443.5	60.5	71.3
Sample II	10 mM CuCl + 8 mM TeO_2	E= -0.5 V	60	735.8	106.6	124.4
Sample III	20 mM CuCl + 8 mM TeO_2	E= -0.5 V	60	1264.1	149.0	186.0
Sample IV	20 mM CuCl + 8 mM TeO_2	E= -0.4 V	60	796.7	101.1	128.1

Due to very few papers reporting AFM data it was quite difficult for comparing our data with similar results that were published earlier. Žalenkiené and Janickis [47-50] have studied the modification of Polyamide 6 film (semi-cristalline polymer named also PA 6 or Nylon 6) by coating with copper chalcogenides in order to change the dielectric properties of this polymer. Layers of

copper sulfide–copper telluride mixture were formed on the PA 6 surface in a chemical procedure by treating with sodium or potassium telluropentathionate ($Na_2TeS_4O_6$, $K_2TeS_4O_6$) solution and then with a solution containing Cu^{2+}/Cu^{+} redox couple and hydroquinone. By applying AFM technique these authors have noticed that the obtained surface was relatively uneven and quite rough. The roughness is modified by increasing the temperature. Sharma et al. [51] have synthesized Cu(I) complexes containing 2-pyridyltellurolate ligands and demonstrated their utility as molecular precursors for preparation of black copper telluride thin films by the aerosol-assisted chemical vapor deposition. XRD patterns have revealed the deposition on glass substrate of cubic $Cu_{1.85}Te$ phase at 350 ^{o}C for 1 h. The AFM images of deposit showed continuous, uniform grains forming a uniform film. Its roughness value was in the range of 16.7-18.3 nm and has increased with deposition time for a particular temperature.

An intercalation of Cu into Te during the electrochemical deposition was performed recently by Huang et al. [52] in trying to demonstrate how the surface properties of Cu_xTe films can be varied quasi-continuously. CuO and TeO_2 were dissolved in $HClO_4$ supporting electrolyte and Au-coated quartz crystal electrode was the working electrode. Comparative AFM images of the obtained Te film and Cu_xTe films with varying compositions ($Cu_{0.55}Te$, $Cu_{1.2}Te$, $Cu_{1.8}Te$) did not show any obvious change in the surface morphology. However, the average grain size has increased if more Cu was intercalated, reaching a doubling of grain size for $Cu_{1.8}Te$ comparing to that on the initial surface of Te film.

In our work the morphological study for scanned fields of 10×10 microns area was performed by recording AFM images. The 2D and 3D views from Figure 10 display comparatively the surfaces of four obtained Cu_xTe films. In general, no major change in the surface morphology of the film can be observed, but more regular grains seem to be for the CuTe samples I and II prepared from 10 mM CuCl + 8 mM TeO_2 composition (both these samples were prepared at -0.5 V). This is confirmed by their topography profiles (not shown here) and is another proof of favorable significant content in Cu_xTe in the detriment of Cu metal for these samples. Instead, the samples from ionic liquid with 20 mM CuCl + 8 mM TeO_2 composition are expected to be Cu-rich Cu_xTe films and their roughness is higher due to more fast growth of copper metal than of Te semi-metal.

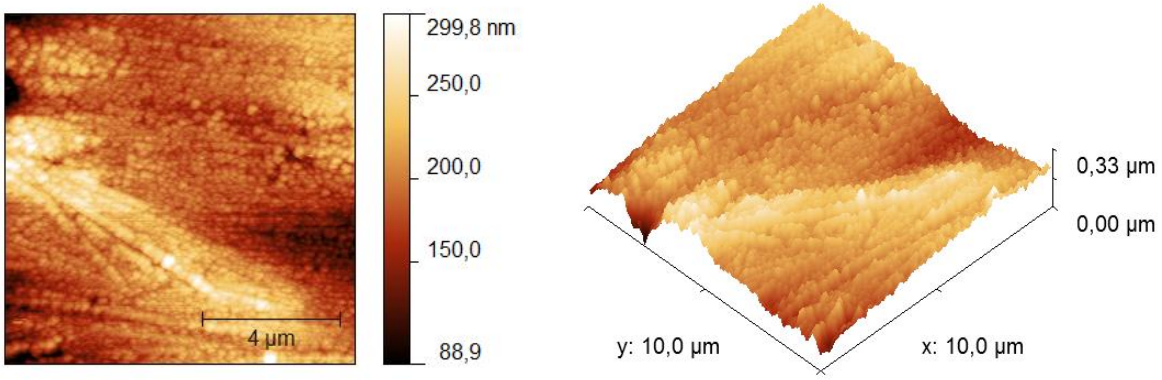

Sample I

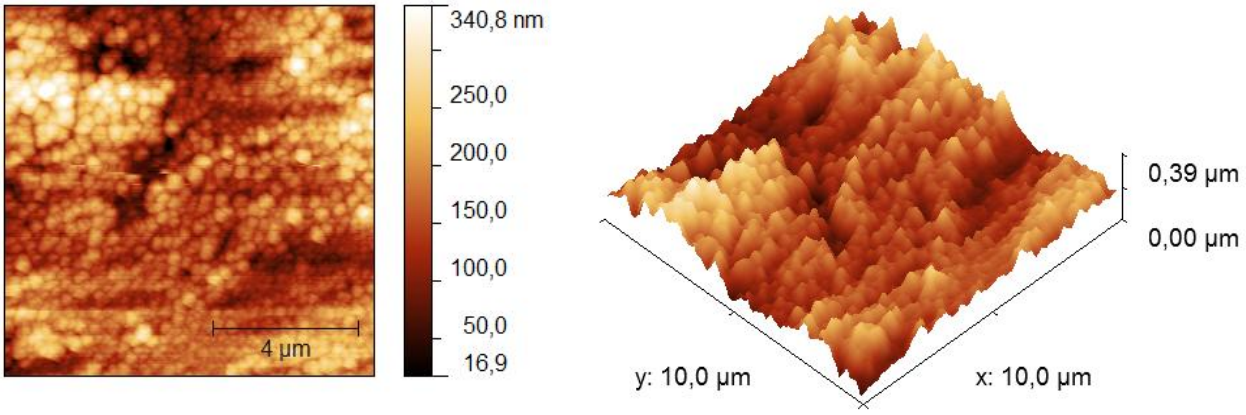

Sample II

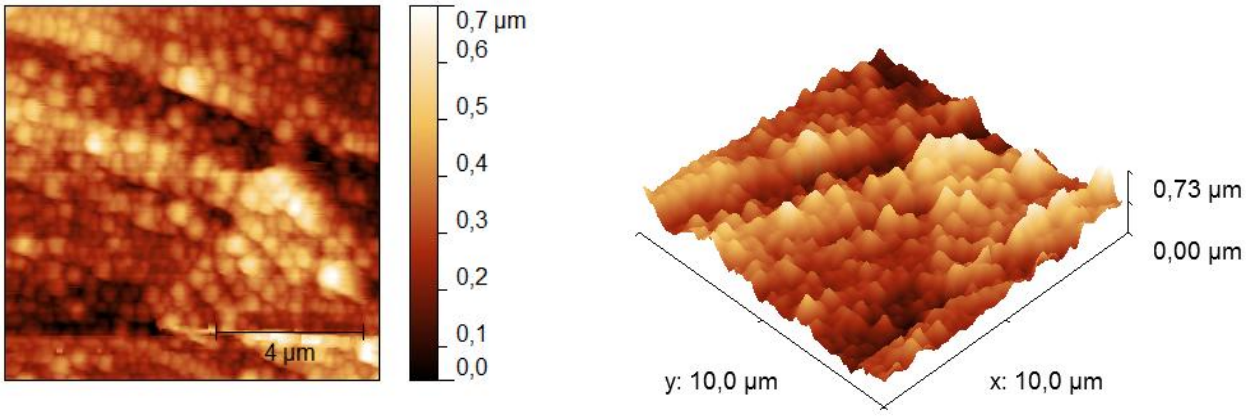

Sample III

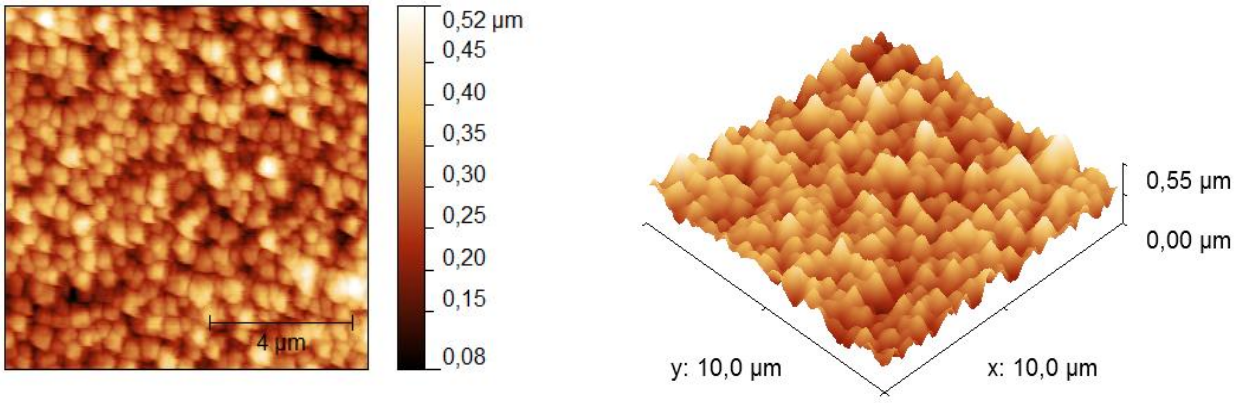

Sample IV

Figure 10. Examples of 2D and 3D AFM images for CuTe films. Electrolysis parameters are given in Table 1

4. CONCLUSIONS

This paper has demonstrated for the first time the possible electrodeposition of copper telluride (Cu_xTe) films on platinum electrode from choline chloride – urea ionic liquid used as solvent. The

shape of cyclic voltammograms suggested that Cu_xTe films were grown on a tellurium coating previously formed by Te-underpotential deposition. The electrochemical investigation showed that the deposition of copper metal is an additional process to the codeposition of copper with tellurium when Cu_xTe compound is formed. The main cathodic process is electrochemically quasireversible and diffusion controlled.

The stoichiometry of copper telluride deposit depends significantly on the electrolyte composition and probably on the polarization potential. Thus, Te rich-deposits of Cu_xTe semiconductor can be prepared from baths with lower Cu^+ content. The preliminary characterization by AFM has showed that film morphologies are dependent on the electrolyte composition and less than the electrolysis time.

ACKNOWLEDGEMENTS
One of the authors recognizes support from the European Social Fund through POSDRU /132395/Inno Research Project implemented in Romania.

References

1. S. Kumar, A. Vohra and S.K. Chakarvarti, *J. Mater. Sci. Mater. Electron.*, 24 (2013) 711.
2. S. Arya, S. Khan, S. Kumar, R. Verma and P. Lehana, *Bull. Mater. Sci.*, 36 (4) (2013) 535.
3. I. Kriegel, J. Rodríguez-Fernandez, A. Wisnet, H. Zhang, C. Waurisch, A. Eychmuller, A. Dubavik,A.O. Govorov and J. Feldmann, *ACS Nano*, 7 (5) (2013) 4367.
4. S. Kumar, V. Singh, A. Vohra and S.K. Chakarvarti, *Amer. J. Mater. Sci. Technol*., 1 (2013) 74.
5. W. Devulder, K. Opsomer, A. Franquet, J. Meersschaut, A. Belmonte, R. Muller, B. De Schutter, S.Van Elshocht, M. Jurczak, L. Goux and C. Detavernier, *J. Appl. Phys.*, 115, (2014) 054501.
6. J. Park, C.K. Lee, K. Kwon and H. Kim, *Int. J. Electrochem. Sci.*, 8 (2013) 4206.
7. T. Ishizaki, D. Yata and A. Fuwa, *Mater. Trans*., 44 (8), (2003) 1583.
8. S. Kumar, V. Kundu, A. Vohra and S.K. Chakarvarti, *J. Mater. Sci. Mater. Electron.*, 22 (2011) 995.
9. S.S. Dhasade, S.H. Han and V.J. Fulari, *J. Semicond.*, 33 (9) (2012) 093002.
10. S. Arya, S. Khan, S. Kumar, R. Verma and P. Lehana, *Bull. Mater. Sci*., 36 (4) (2013) 535.
11. S.Kumar, A. Vohra and S.K. Chakarvarti, *Nanomater. Nanotechnol.*, 2 (2012), Art.3:2012.
12. E. Rudnik and J. Kozłowski, *Electrochim. Acta*, 107 (2013) 103.
13. S. López-León, R. Ortega-Borges and G. Brisard, *Int. J. Electrochem. Sci.*, 8 (2013) 1382.
14. Y. Yang, C. Xu, Y. Hua, J. Li, F. Li and Y. Jie, *Int. J. Electrochem. Sci.*, 10 (2015) 1979.
15. J. Park, Y. Jung, P. Kusumah, J. Lee, K. Kwon and C.K. Lee, *Int. J. Mol. Sci.*, 15 (9) (2014) 15320.
16. S. Zein El Abedin, A.Y. Saad, H.K. Farag, N. Borisenko, Q.X. Liu and F. Endres, *Electrochim.Acta*, 52 (2007) 2746.
17. S. Zein El Abedin, A. Prowald and F. Endres, *Electrochem. Commun.*, 18 (2012) 70.
18. P.Y. Chen and Y.T. Chang, *Electrochim. Acta*, 75 (2012) 339.
19. P. Yang, Y. Zhao, C. Su, K. Yang, B. Yan and M. An, *Electrochim. Acta* 88, (2013) 203.
20. G. Saravanan and S. Mohan, *New J. Chem.*, 37 (8) (2013) 2564.
21. T. Vainikka, D. Lloyd, L. Murtomaki, J.A. Manzanares and K. Kontturi, *Electrochim. Acta*, 8 (2013) 739.
22. T. Liu, R. Vilar, S. Eugenio, J. Grondin and Y. Danten, *J. Appl. Electrochem.*, 44 (1) (2014) 189.
23. T. Liu, R. Vilar, S. Eugenio, J. Grondin and Y. Danten, *J. Appl. Electrochem.*, 45 (2015) 87.

24. S. Vanderaspoilden, J. Christophe, Th. Doneux and C. Buess-Herman, *Electrochim. Acta*,162 (2015) 156.
25. F. Golgovici, A. Cojocaru, M. Nedelcu and T. Visan, *Chalcog. Lett.*, 6 (8) (2009) 323.
26. F. Golgovici, A. Cojocaru, C. Agapescu, Y. Jin, M. Nedelcu, W. Wang and T. Visan, *Studia Univ.Babes-Bolyai, Chemia*, 54 (Spec. Issue 1) (2009) 175.
27. F. Golgovici, A. Cojocaru, M. Nedelcu and T. Visan, *J. Electron. Mater.*, 39 (9) (2010) 2079.
28. F. Golgovici, A. Cojocaru, L. Anicai and T. Visan, *Mater. Chem. Phys.*, 126 (3) (2011) 700.
29. F. Golgovici and T. Visan, *Chalcog. Lett*., 8 (2011) 487.
30. F. Golgovici and T. Visan, *Chalcog. Lett.*, 9 (4) (2012) 165.
31. M.L. Mares, F. Golgovici and T. Visan, *Chalcog. Lett.*, 10 (8) (2013) 259.
32. C. Agapescu, A. Cojocaru, A. Cotarta and T. Visan, *J. Appl. Electrochem*, 43 (3) (2013) 309.
33. E. Gómez and E. Vallés, *Int. J. Electrochem. Sci.*, 8 (2013) 1443.
34. B.P. Pollet, J.-Y. Hihn and T.J. Mason, *Electrochim. Acta*, 53 (12) (2008) 4248.
35. T.I. Leong, I.W. Sun, M.J. Deng, C.M. Wu and P.Y. Chen, *J. Electrochem. Soc.*, 155(4) (2008)F55.
36. P.Y. Chen, M.J. Deng and D.X. Zhuang, *Electrochim. Acta*, 54 (27) (2009) 6935.
37. J.K. Chang, *Electrochem.*, 77 (2009) 582.
38. A.M. Popescu, V. Constantin, A. Cojocaru and M. Olteanu, *Rev. Chim. (Bucharest)*, 62 (2) (2011)206.
39. A.M. Popescu, V. Constantin, M. Olteanu, O. Demidenko and K. Yanushkevich, *Rev. Chim. (Bucharest)* 62 (6) (2011) 626.
40. C.D. Gu, Y.H. You, X.L. Wang and J.P. Tu, *Surf. Coat. Technol.*, 209 (2012) 117.
41. A.M. Popescu, A. Cojocaru, C. Donath and V. Constantin, *Chem. Res. Chinese Univ.*, 29 (5)(2013) 991.
42. S. Xing, C. Zanella and F. Deflorian, *J. Solid State Electrochem.*, 18 (6) (2014) 1657.
43. A. Mandroyan, M. Mourad-Mahmoud, M,-L. Doche and J.-Y. Hihn, *Ultrasonics Sonochem.*, 21 (6) (2014) 2010.
44. S. Ghosh and S. Roy, *Surf. Coat. Technol.*, 238 (2014) 165.
45. D. Yue, Y. Jia, Y. Yao, J. Sun and Y. Jing, *Electrochim. Acta*, 65 (2012) 30.
46. M.L. Mares Badea, A. Cojocaru and L. Anicai, *U.P.B. Sci. Bull., Series B*, 76 (3) (2014) 21.
47. S. Žalenkienė and V. Janickis, *Chemija*, 21 (2-4) (2010) 89.
48. J. Šukyto, S. Žalenkienė and V. Janickis, *Mater. Sci. (Medziagotyra)*, 16 (2) (2010) 108.
49. V. Janickis and S. Žalenkienė, *Open Chem*., 8 (4) (2010) 709.
50. S. Žalenkienė and V. Janickis, *Mater. Sci. (Medziagotyra)*, 18 (2) (2012) 112.
51. R.K. Sharma, G. Kedarnath, V.K. Jain, A. Wadawale, C.G.S. Pillai, M. Nalliath and B.Vishwanadh, *Dalton Trans.*, 40 (2011) 9194.
52. M. Huang, A. Maljusch, F. Calle-Vallejo, J.B. Henry, M.T.M. Koper, W. Schuhmann, A.S. Bondarenko, *RSC Adv.*, 3 (2013) 21648.